END

DATE
FILMED

3-77

1.0

2.8   2.5

3.2   2.2

3.6

4.0   2.0

1.1

1.8

1.25   1.4   1.6

MICROCOPY RESOLUTION TEST CHART
NATIONAL BUREAU OF STANDARDS-1963-

RADC-TR-77-34
Phase Report
January 1977

POINT SOURCE REPRESENTATION OF ANTENNAS AND OBSTACLES

Syracuse University

D D C

FEB 28 1977

Approved for public release;
distribution unlimited.

This report has been reviewed by the RADC Information Office (OI) and is releasable to the National Technical Information Service (NTIS). At NTIS it will be releasable to the general public, including foreign nations.

This report has been reviewed and approved for publication.

APPROVED: *Jacob Scherer*

JACOB SCHERER
Project Engineer

APPROVED: *Joseph J. Naresky*

JOSEPH J. NARESKY
Chief, Reliability and Compatibility Division

FOR THE COMMANDER: *John P. Huss*

JOHN P. HUSS
Acting Chief, Plans Office

REPORT DOCUMENTATION PAGE

READ INSTRUCTIONS
BEFORE COMPLETING FORM

1. REPORT NUMBER	2. GOVT ACCESSION NO.	3. RECIPIENT'S CATALOG NUMBER
RADC-TR-77-34		

4. TITLE (and Subtitle)	5. TYPE OF REPORT & PERIOD COVERED
POINT SOURCE REPRESENTATION OF ANTENNAS AND OBSTACLES	Phase Report,
	6. PERFORMING ORG. REPORT NUMBER
	N/A

7. AUTHOR(s)	8. CONTRACT OR GRANT NUMBER(s)
Dr. Jose Perini	F30602-75-C-0121
Dr. Jason Chou	

9. PERFORMING ORGANIZATION NAME AND ADDRESS	10. PROGRAM ELEMENT, PROJECT, TASK AREA & WORK UNIT NUMBERS
Syracuse University	95670016
Syracuse NY 13210	

11. CONTROLLING OFFICE NAME AND ADDRESS	12. REPORT DATE
Rome Air Development Center (RBC)	Jan 77
Griffiss AFB NY 13441	13. NUMBER OF PAGES
	23

14. MONITORING AGENCY NAME & ADDRESS(if different from Controlling Office)	15. SECURITY CLASS. (of this report)
Same	UNCLASSIFIED
	15a. DECLASSIFICATION/DOWNGRADING SCHEDULE
	N/A

16. DISTRIBUTION STATEMENT (of this Report)

Approved for public release; distribution unlimited.

no. P.E. no given

17. DISTRIBUTION STATEMENT (of the abstract entered in Block 20, if different from Report)

Same

18. SUPPLEMENTARY NOTES
RADC Project Engineer: Jacob Scherer (RBC)

19. KEY WORDS (Continue on reverse side if necessary and identify by block number)
Electromagnetic Compatibility
Electromagnetic Fields
Antennas
Method of Moments

20. ABSTRACT (Continue on reverse side if necessary and identify by block number)
In this report the behavior of the current on a parasite wire as a function of the distance d from the driven wire has been investigated for d in the range from .1λ to 2λ. The mutual coupling presented by adjacent parasite wires has been taken into account. The result shows that the parasite wire current magnitude and phase can be predicted by a simple relation.

Lambda

DD FORM 1473   EDITION OF 1 NOV 69 IS OBSOLETE
1 JAN 73

REPORT DOCUMENTATION PAGE

PREFACE

This effort was conducted by Syracuse University under the sponsorship of the Rome Air Development Center Post-Doctoral Program for NAVSEC. Mr. Tony Testa of NAVSEC was the task project engineer and provided overall technical direction and guidance. The authors of this report are Dr. Jose Perini and Jason Chou.

The RADC Post-Doctoral Program is a cooperative venture between RADC and some sixty-five universities eligible to participate in the program. Syracuse University (Department of Electrical and Computer Engineering), Purdue University (School of Electrical Engineering), Georgia Institute of Technology (School of Electrical Engineering), and State University of New York at Buffalo (Department of Electrical Engineering) act as prime contractor schools with other schools participating via sub-contracts with the prime schools. The U.S. Air Force Academy (Department of Electrical Engineering), Air Force Institute of Technology (Department of Electrical Engineering), and the Naval Post Graduate School (Department of Electrical Engineering) also participate in the program.

The Post-Doctoral Program provides an opportunity for faculty at participating universities to spend up to one year full time on exploratory development and problem-solving efforts with the post-doctorals splitting their time between the customer location and their educational institutions. The program is totally customer-funded with current projects being undertaken for Rome Air Development Center (RADC),

Space and Missile Systems Organization (SAMSO), Aeronautical Systems Division (ASD), Electronic Systems Division (ESD), Air Force Avionics Laboratory (AFAL), Foreign Technology Division (FTD), Air Force Weapons Laboratory (AFWL), Armament Development and Test Center (ADTC), Air Force Communications Service (AFCS), Aerospace Defense Command (ADC), Hq USAF, Defense Communications Agency (DCA), Navy, Army, Aerospace Medical Division (AMD), and Federal Aviation Administration (FAA).

Further information about the RADC Post-Doctoral Program can be obtained from Jacob Scherer, RADC/RBC, Griffiss AFB, NY, 13441, telephone AV 587-2543, COMM (315) 330-2543.

TABLE OF CONTENTS

LIST OF FIGURES

POINT SOURCE REPRESENTATION OF ANTENNAS AND OBSTACLES

1. Introduction

In the report "Point Source Radiation Pattern Synthesis by Iterative Techniques" [1] a method was presented to synthesize radiation patterns of planar arrays of point sources. More recently Raschke and Sterling [2] have proposed the idea of representing the superstructure elements of a ship such as deck houses, stacks, fences, etc., by vertical wires. One of the authors [3] has then suggested that all antennas and wires be represented by an equivalent point source and the techniques used in [1] be applied to the problem of optimally locating antennas aboard ships.

The difficulty of this approach is that in order to obtain the point source representation of the wires and antennas, the entire problem has to be solved by some technique such as the Method of Moments (MOM) for every iteration. If the total number of wires is large, then the procedure becomes very costly in computer time and may preclude the solution of the problem.

The purpose of this report is to investigate a possible simplification of the above problem by making the hypothesis that "all wires of the same obstacle will have current distributions which are essentially of the same shape. They will differ in magnitude by a factor $K\lambda/d$ and in phase by $2\pi d/\lambda$" If this is true, it will only be necessary at the beginning of the iterative procedure to solve the considerably smaller MOM problem of the antennas to be located and one "typical" wire for each obstacle present. The currents in all other wires of the same obstacle will then be derived from the "typical" one by the above hypothesized relations. This will continue throughout the

1

synthesis procedure. At the end, the problem can be resolved by MOM again to check the accuracy of the result. If necessary, the recomputed typical currents can be used as a starting point for a few more iterations.

2. Antenna with Obstacle

A situation often encountered in shipboard antenna design problems is that of an antenna in front of a deck-house as shown in Fig. 1. The whole structure will initially be assumed over an infinite perfect ground plane.

To simplify the treatment of these problems, Raschke and Sterling [2] made the hypotheses that (a) only the conducting plate facing the antenna is important, and (b) this plate may be represented by a set of equally spaced parallel wires (parasite wires) as shown in Fig. 2.

The parasite wire length L is the same as the height of the plate. The spacing s between adjacent wires should be chosen as large as possible to reduce the computation work. Yet it cannot be so large as to become a poor representation of the plate. Previous experience has shown that s = $\lambda/8$ yields good results.

The current induced in each wire when the antenna is driven can be accurately calculated by the method of moments (MOM). However, if this approach is used in the problem of locating shipboard antennas, one execution of a MOM algorithm is required at each iteration step. This is expensive and unnecessary since approximate currents for the intermediate iteration steps will serve as well.

In the next two sections, we propose a simple relation to obtain approximate parasite currents for any value of d, the distance from the antenna to the parasite wires.

2
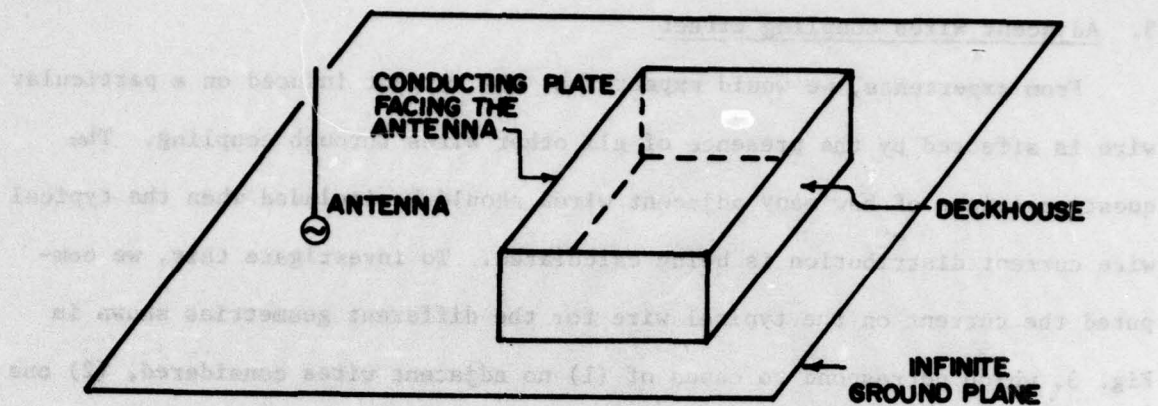
FIG. I AN ANTENNA IN FRONT OF A DECKHOUSE
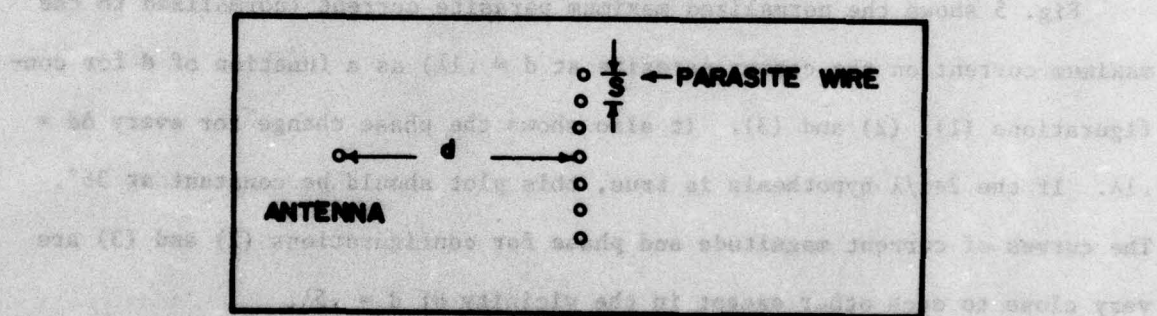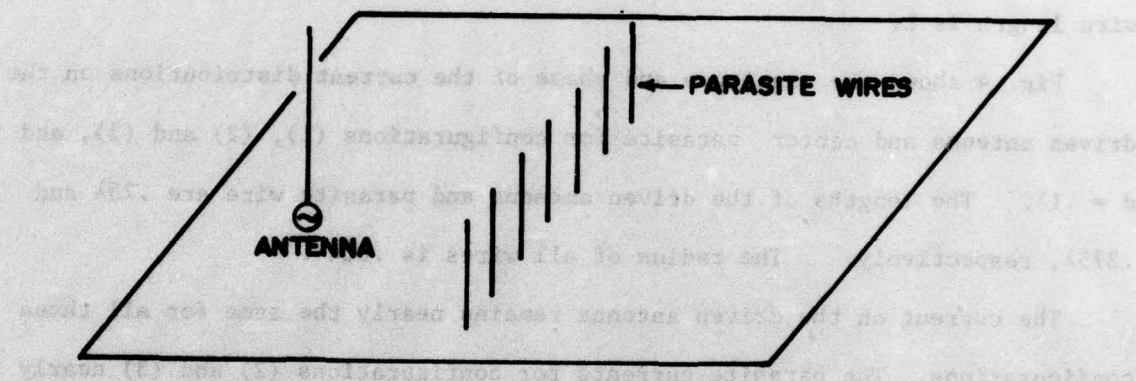
FIG. 2 ANTENNA WITH PARASITE WIRES

3. Adjacent Wires Coupling Effect

From experience, we would expect that the current induced on a particular wire is affected by the presence of all other wires through coupling. The question arises of how many adjacent wires should be included when the typical wire current distribution is being calculated. To investigate this, we computed the current on the typical wire for the different geometries shown in Fig. 3, which correspond to cases of (1) no adjacent wires considered, (2) one adjacent wire on each side, and (3) two adjacent wires on each side. The distance from a driven antenna to the center parasite wire is d and the parasite wire length is L.

Fig. 4 shows the magnitude and phase of the current distributions on the driven antenna and center parasite for configurations (1), (2) and (3), and $d = .1\lambda$. The lengths of the driven antenna and parasite wire are $.25\lambda$ and $.375\lambda$, respectively. The radius of all wires is $.004\lambda$.

The current on the driven antenna remains nearly the same for all three configurations. The parasite currents for configurations (2) and (3) nearly coincide with each other.

Fig. 5 shows the normalized maximum parasite current (normalized to the maximum current on the center parasite at $d = .1\lambda$) as a function of d for configurations (1), (2) and (3). It also shows the phase change for every $\Delta d = .1\lambda$. If the $2\pi d/\lambda$ hypothesis is true, this plot should be constant at 36°. The curves of current magnitude and phase for configurations (2) and (3) are very close to each other except in the vicinity of $d = .5\lambda$.

The same procedure was used for the case of the parasite wires of length $.325\lambda$ and the results are shown in Figs. 6 and 7.

4

STUDY OF PARASITE ANTENNA CURRENT
ALL WIRE RADIUS = .004λ
L = (A) .375λ   (B) .325λ
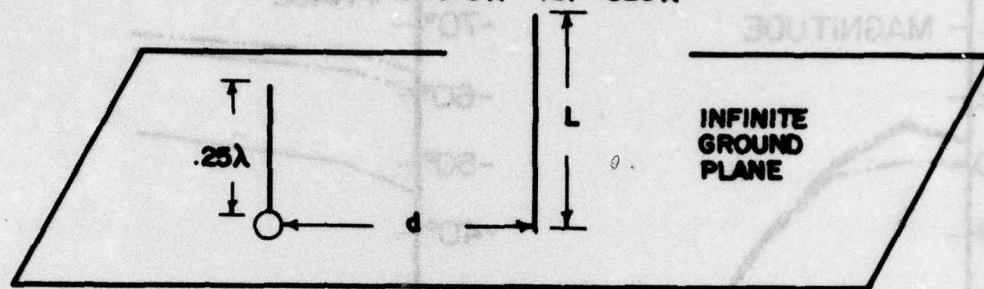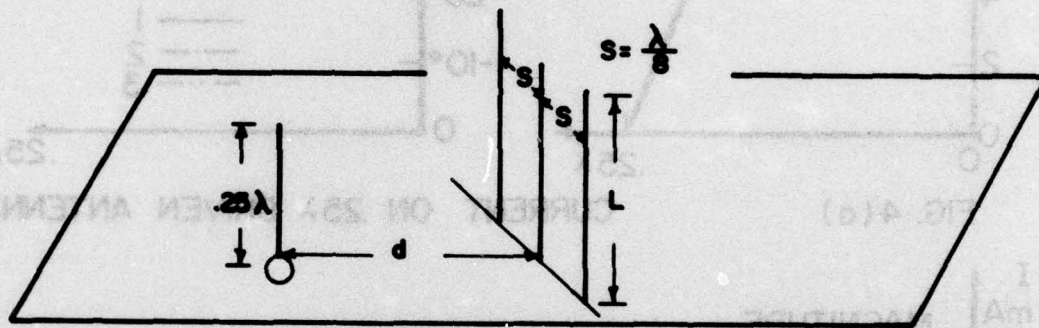
(a)   CONFIGURATION (1)

(b)   CONFIGURATION (2)
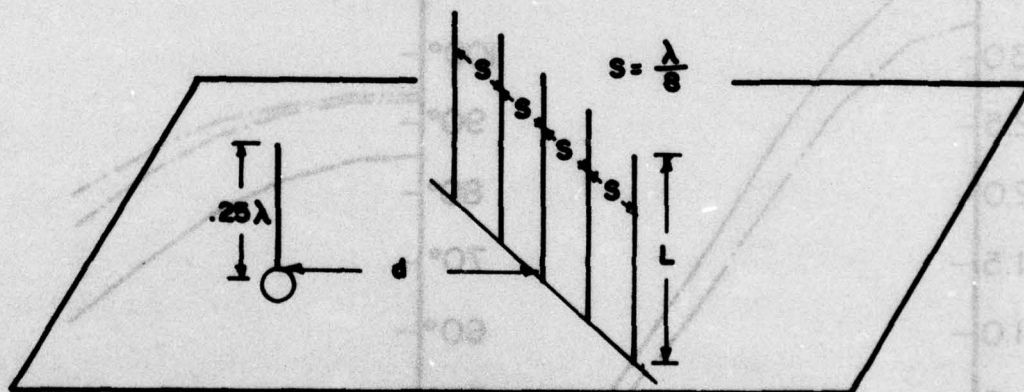
(c)   CONFIGURATION (3)

FIG. 3   ADJACENT WIRE COUPLING BY DIFFERENT GEOMETRY

5

FIG. 4(a)   CURRENT ON 25λ DRIVEN ANTENNA

FIG. 4(b)   CURRENT ON .375λ PARASITE WIRE
                   d =.1λ

6

FIG. 5 NORMALIZED MAXIMUM PARASITE CURRENT AND PHASE
AS A FUNCTION OF d/λ

7

FIG. 6(a) CURRENT ON .25 λ DRIVEN ANTENNA

FIG. 6(b) CURRENT ON .325 λ PARASITE WIRE d = .1λ
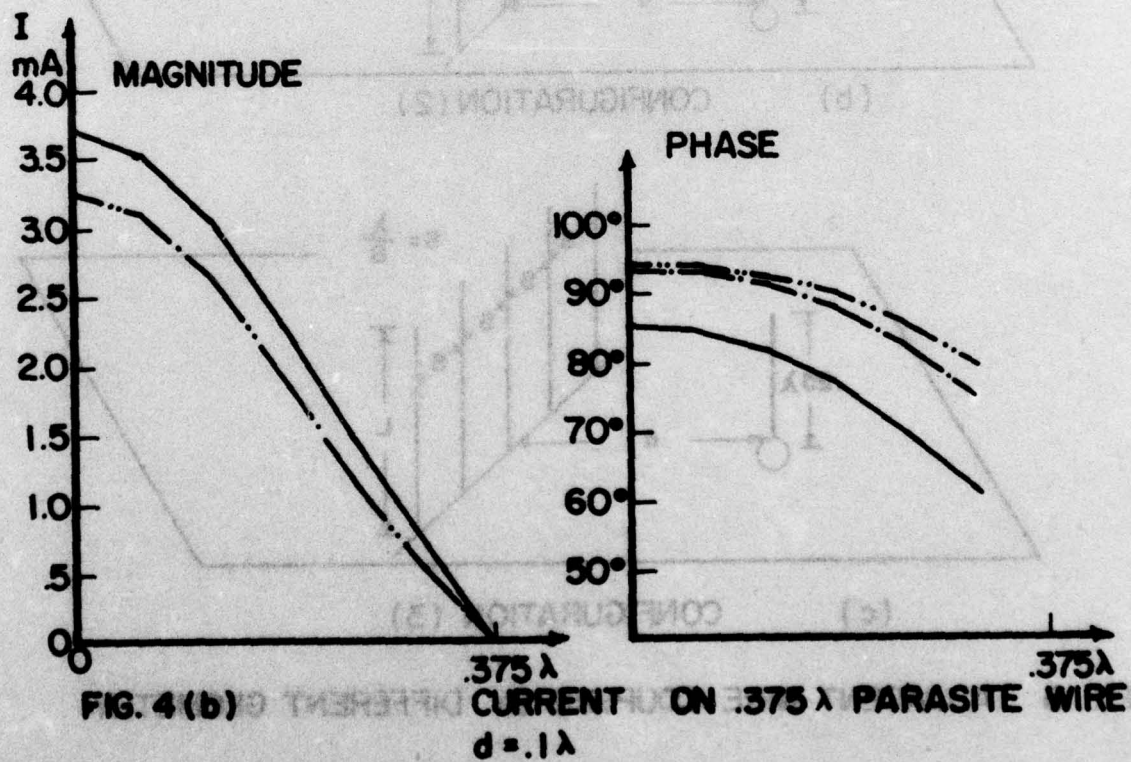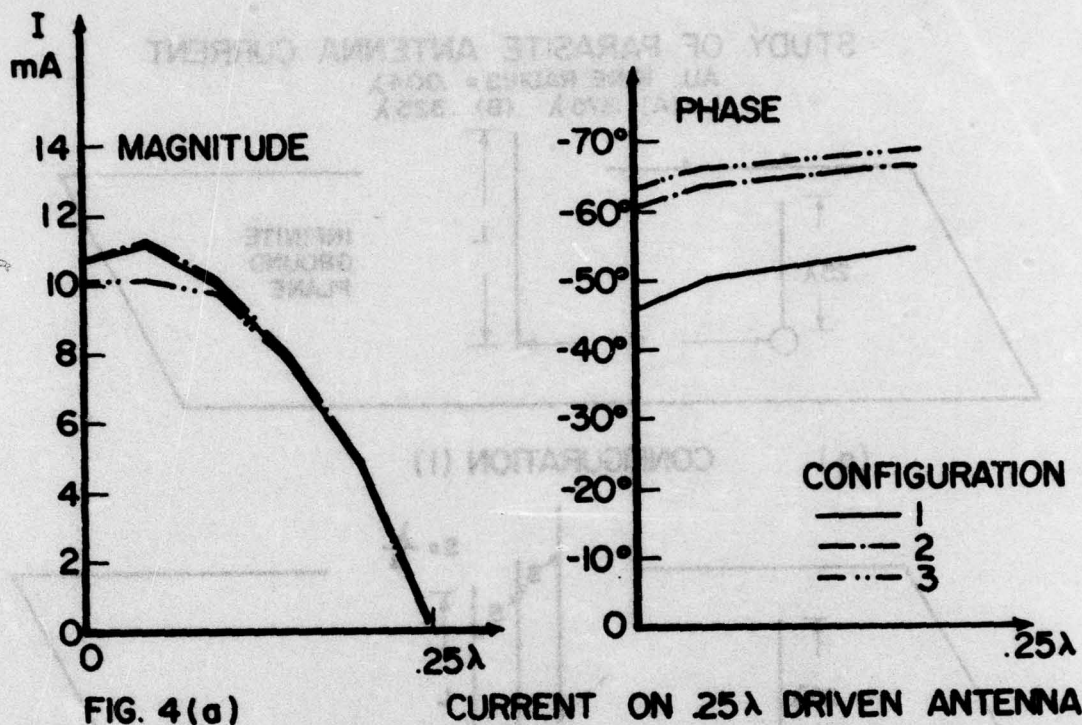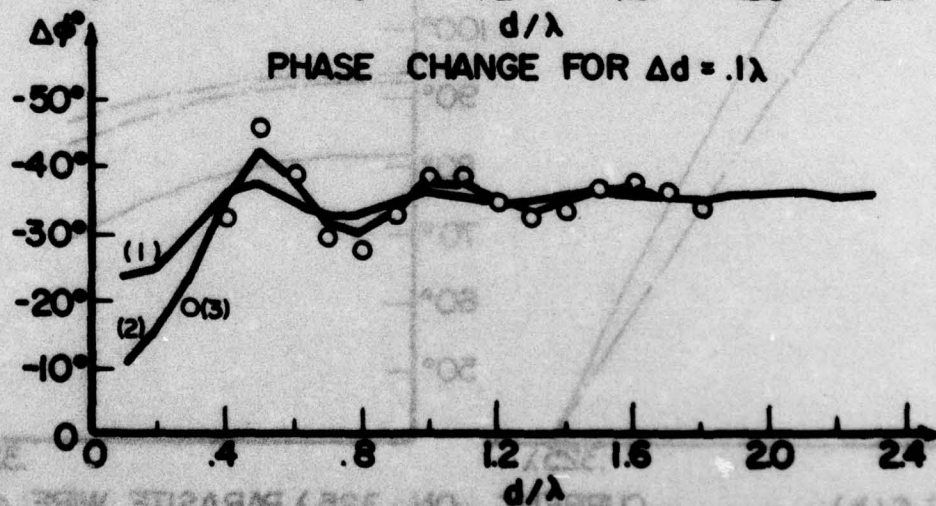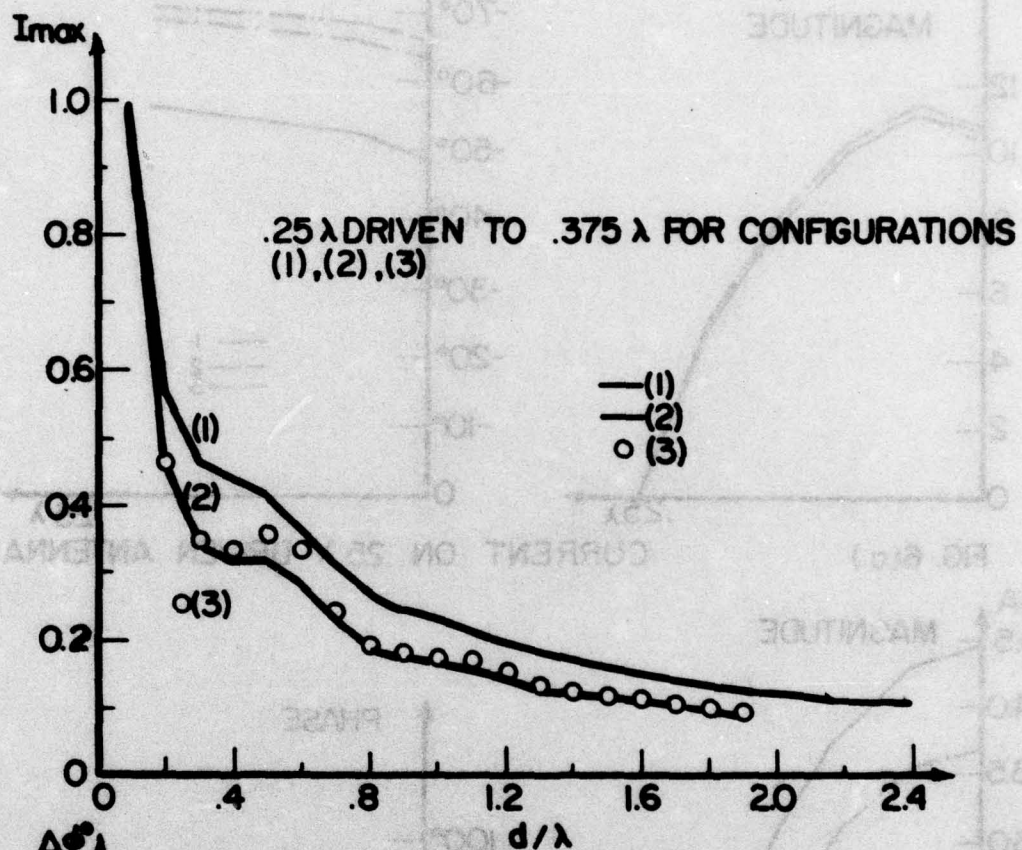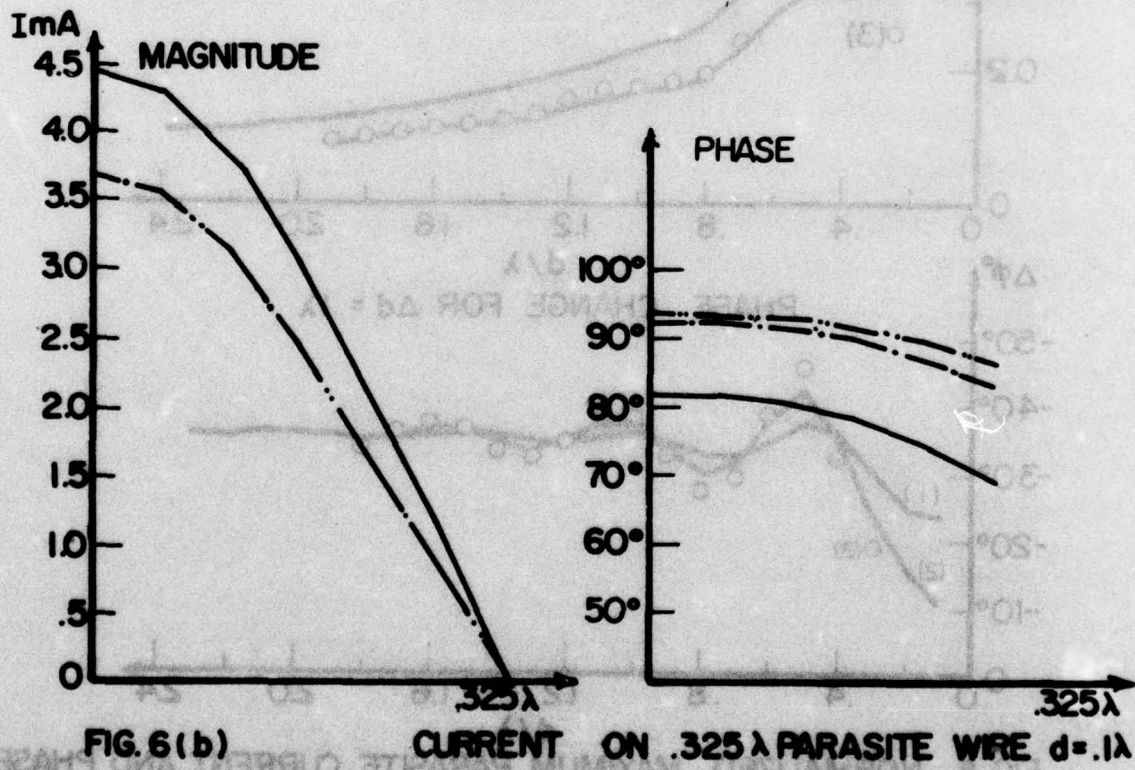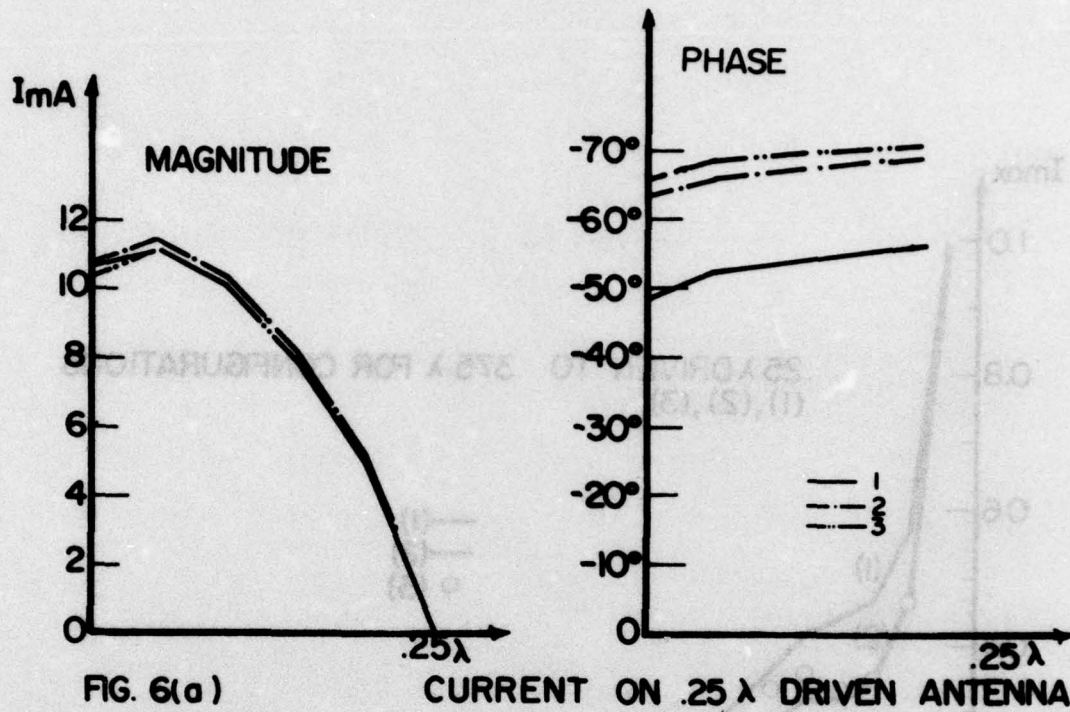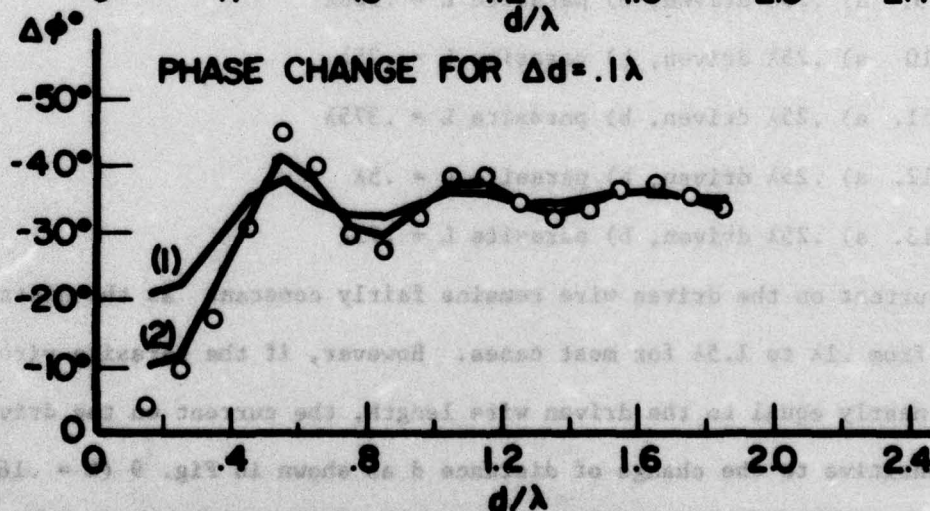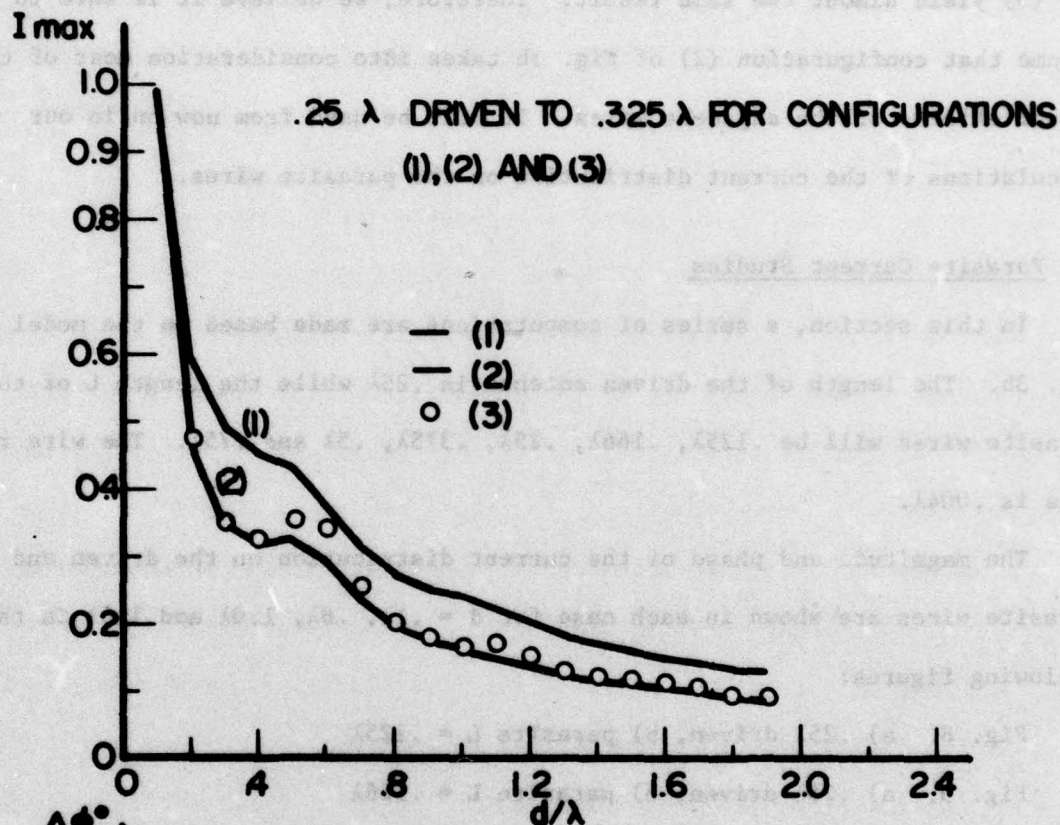
FIG. 7 NORMALIZED MAXIMUM PARASITE CURRENT AND PHASE AS A FUNCTION OF d/λ

9

It is observed from Figs. 4 through Fig. 7 that the configurations (2) and (3) yield almost the same result. Therefore, we believe it is safe to assume that configuration (2) of Fig. 3b takes into consideration most of the mutual effects of the adjacent wires. It will be used from now on in our calculations of the current distribution on the parasite wires.

4. Parasite Current Studies

In this section, a series of computations are made based on the model of Fig. 3b. The length of the driven antenna is $.25\lambda$ while the length L of the parasite wires will be $.125\lambda$, $.166\lambda$, $.25\lambda$, $.375\lambda$, $.5\lambda$ and $.75\lambda$. The wire radius is $.004\lambda$.

The magnitude and phase of the current distribution on the driven and parasite wires are shown in each case for $d = .1\lambda$, $.6\lambda$, 1.0λ and 1.5λ in the following figures:

Fig. 8. a) $.25\lambda$ driven, b) parasite $L = .125\lambda$

Fig. 9. a) $.25\lambda$ driven, b) parasite $L = .166\lambda$

Fig. 10 a) $.25\lambda$ driven, b) parasite $L = .25\lambda$

Fig. 11. a) $.25\lambda$ driven, b) parasite $L = .375\lambda$

Fig. 12. a) $.25\lambda$ driven, b) parasite $L = .5\lambda$

Fig. 13. a) $.25\lambda$ driven, b) parasite $L = .75\lambda$

The current on the driven wire remains fairly constant as the distance d changes from $.1\lambda$ to 1.5λ for most cases. However, if the parasite wire length is nearly equal to the driven wire length, the current on the driven wire is sensitive to the change of distance d as shown in Fig. 9 ($L = .166\lambda$) and Fig. 10 ($L = .25\lambda$).

The magnitude and phase distribution for the parasite wire current is

10
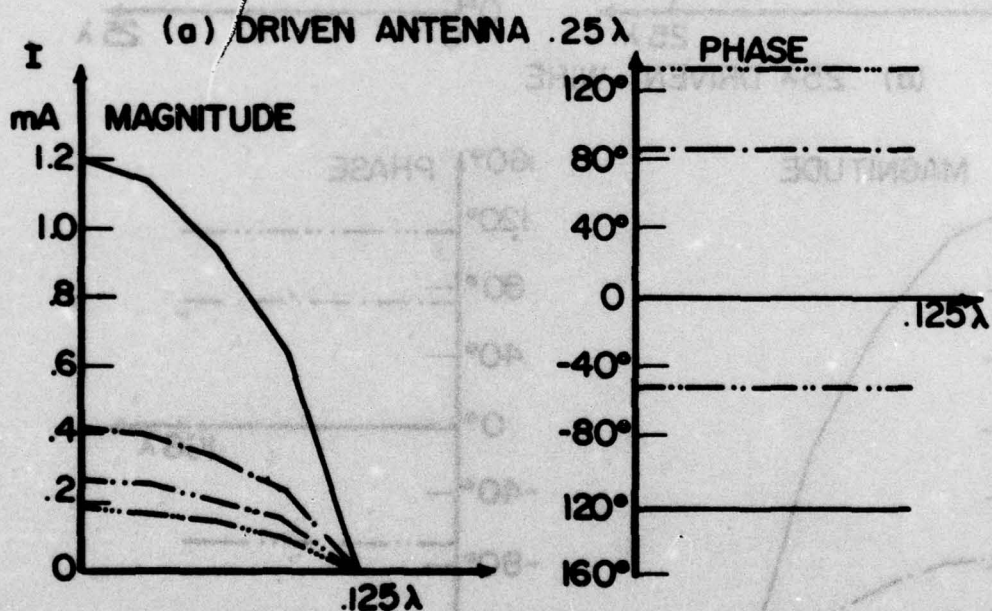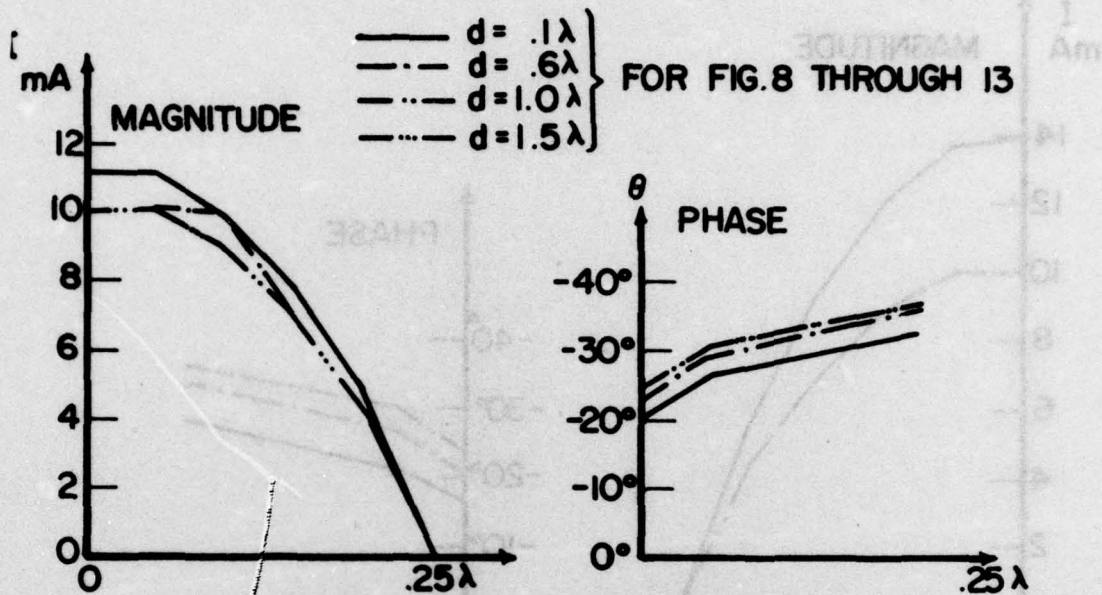
FIG.8 CURRENT DISTRIBUTION .25λ TO .125λ

11
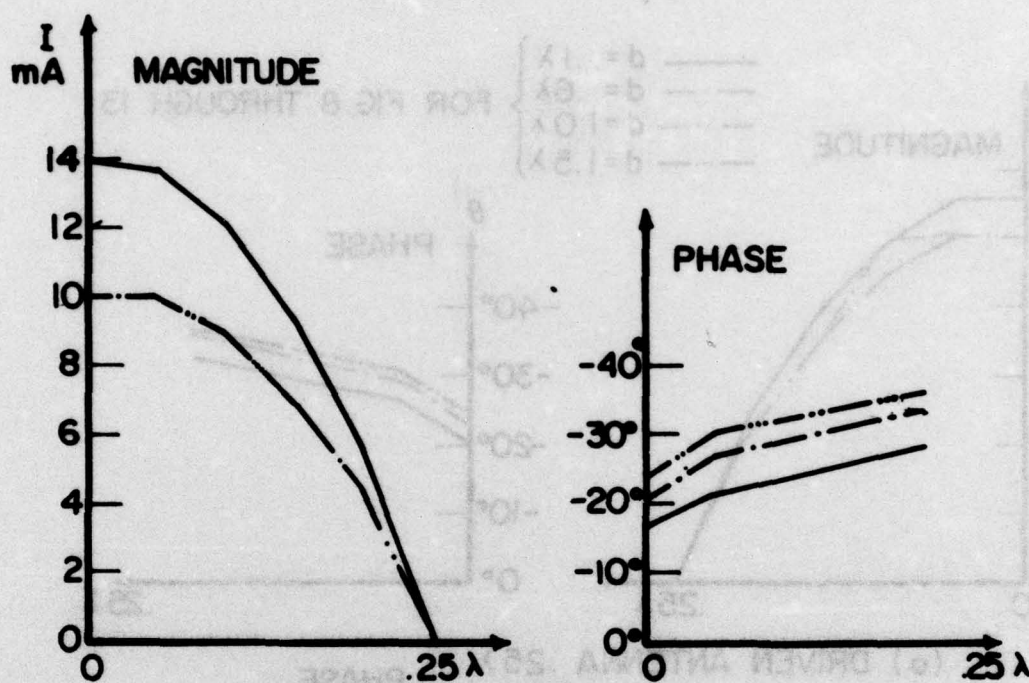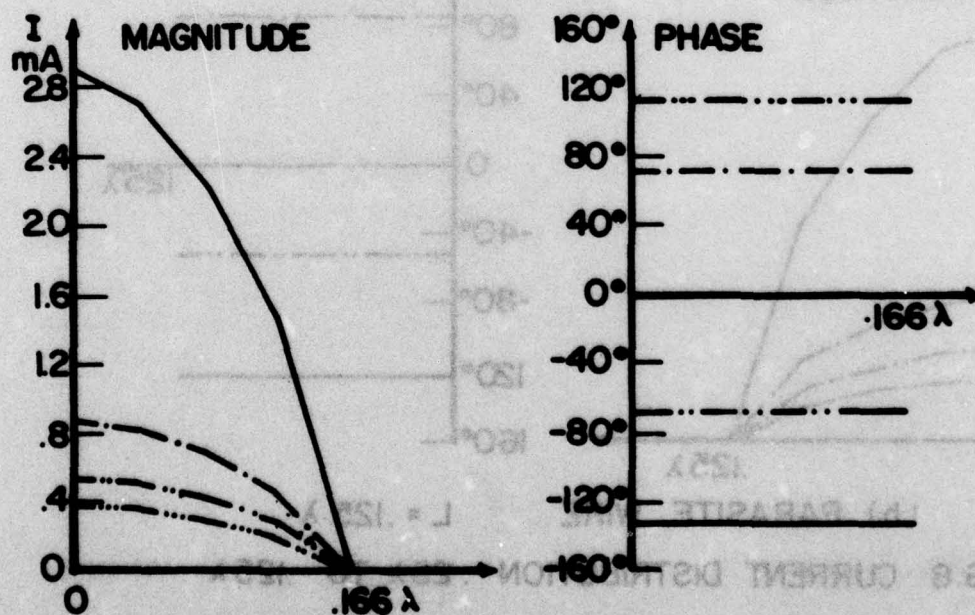
(a) .25λ DRIVEN WIRE

(b) .166λ PARASITE WIRE
FIG. 9 CURRENT DISTRIBUTION .25λ TO .166λ
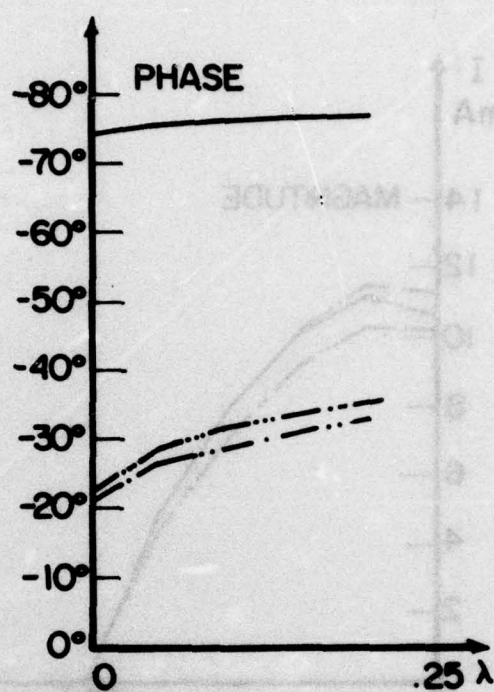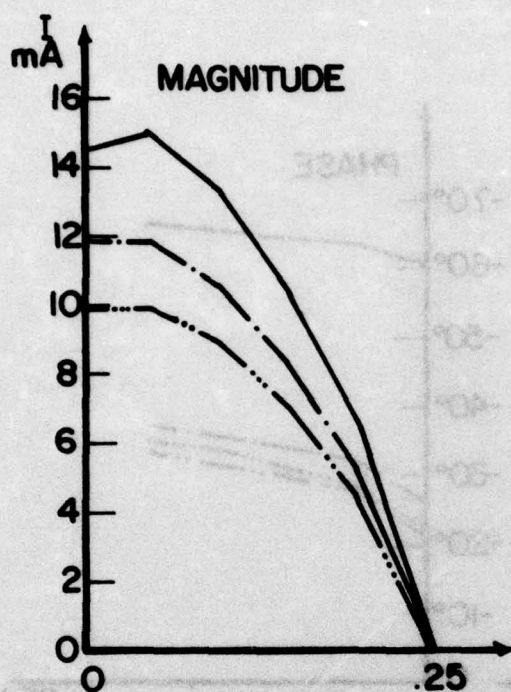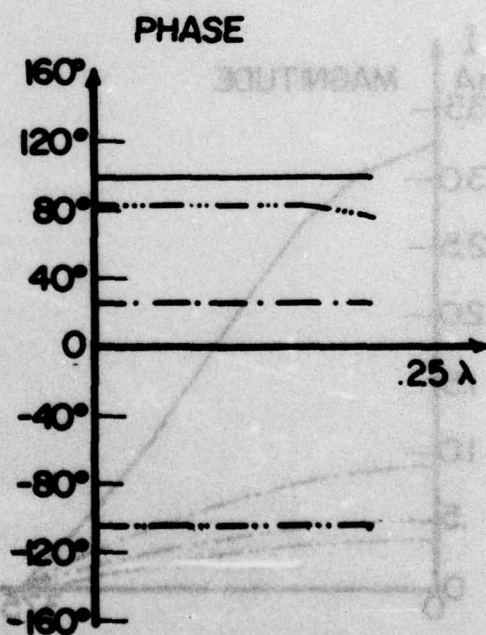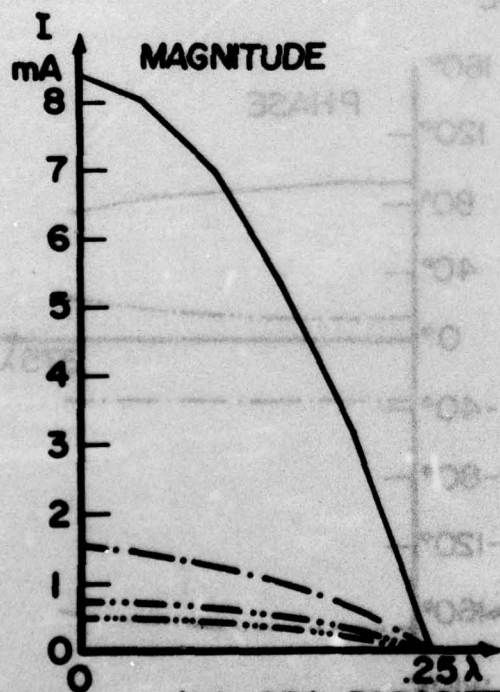
12

FIG.10   CURRENT DISTRIBUTION .25 λ TO .25 λ

(a) .25λ DRIVEN WIRE

(b) .375 λ PARASITE WIRE

FIG. II   CURRENT DISTRIBUTION .25λ TO .375λ

14

(a) .25λ DRIVEN WIRE

(b) .5λ PARASITE WIRE

FIG. 12 CURRENT DISTRIBUTION .25λ TO .5λ

15

I ▲ MAGNITUDE   PHASE
mA

14

12
10
 8
 6
 4
 2
 0   0
   0   .25   .25λ
        (a) .25 λ DRIVEN WIRE

-70°
-60°
-50°
-40°
-30°
-20°
-10°

I
mA   MAGNITUDE   PHASE

2.8   120°
2.4   80°
2.0   40°
1.6   0°
1.2   -40°
 .8   -80°
 .4   -120°
 0   .75λ
        (b) .75 λ PARASITE WIRE
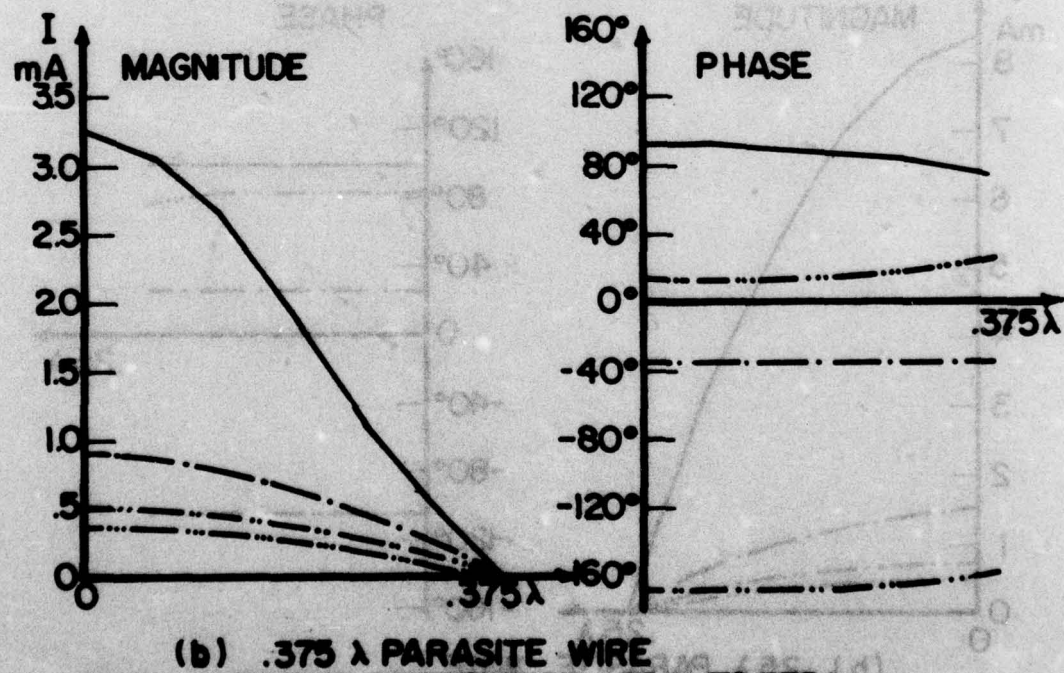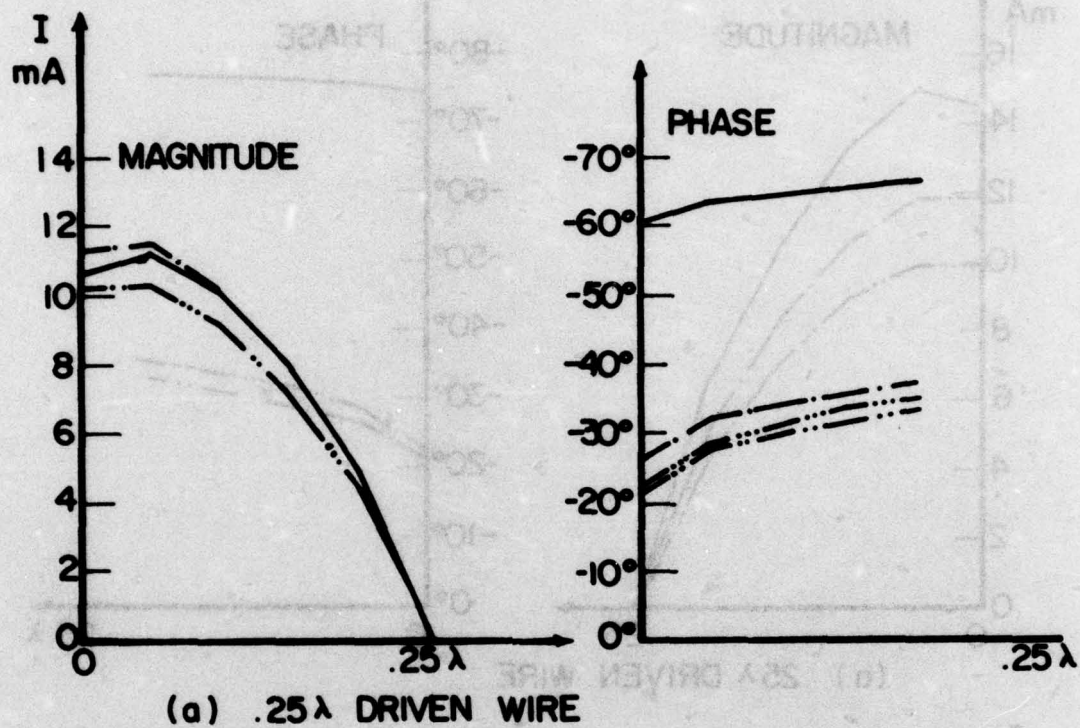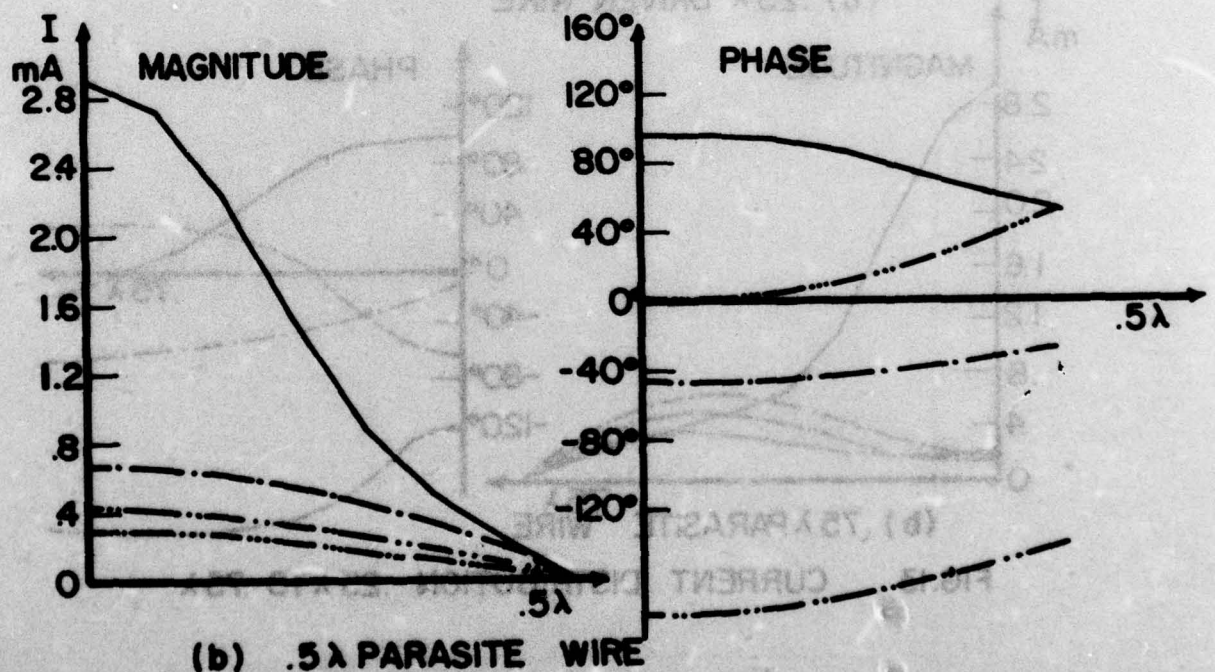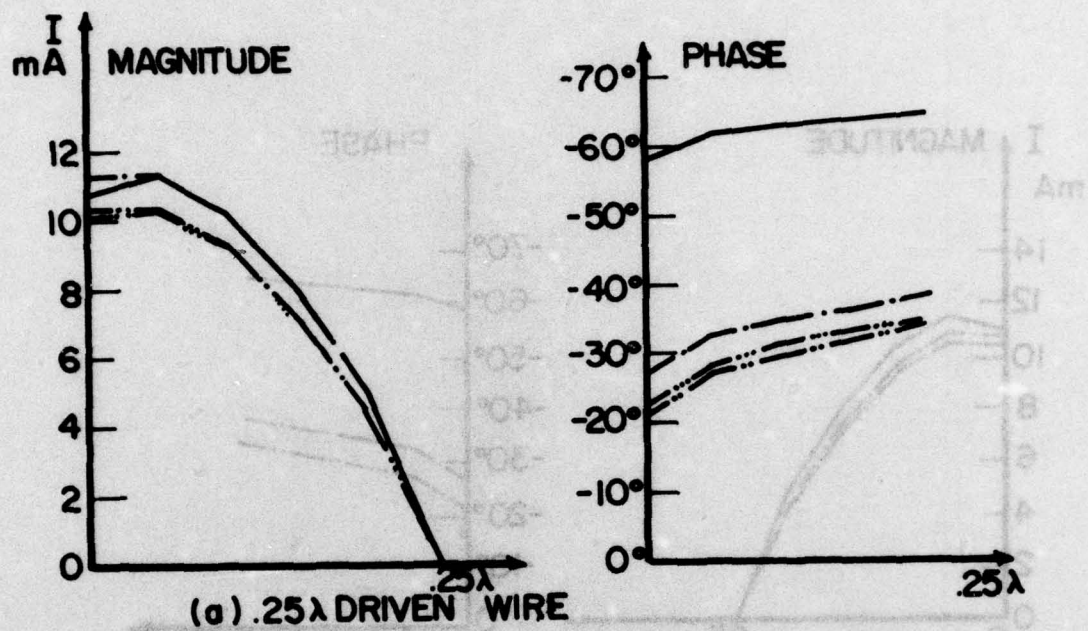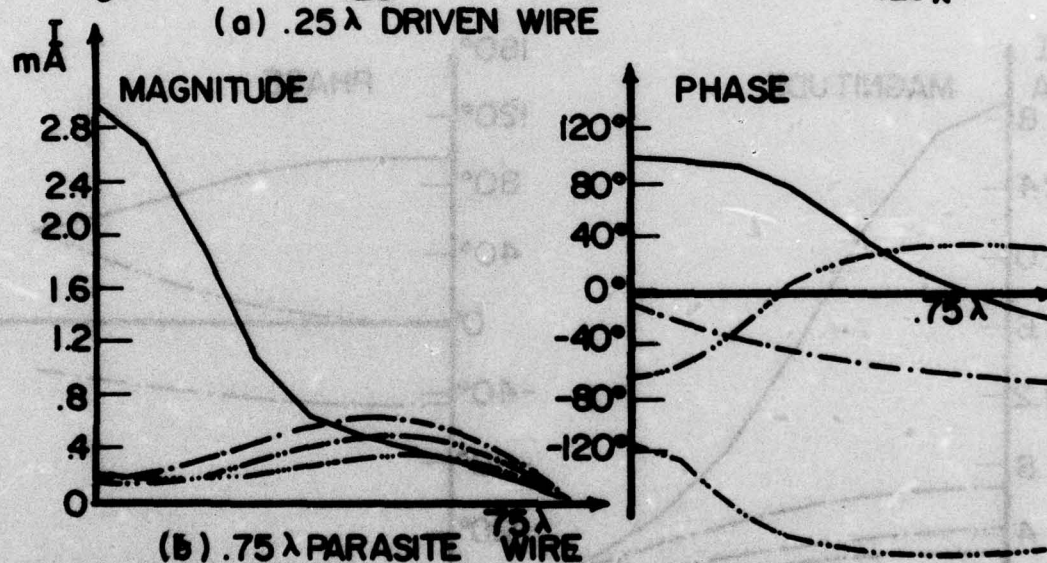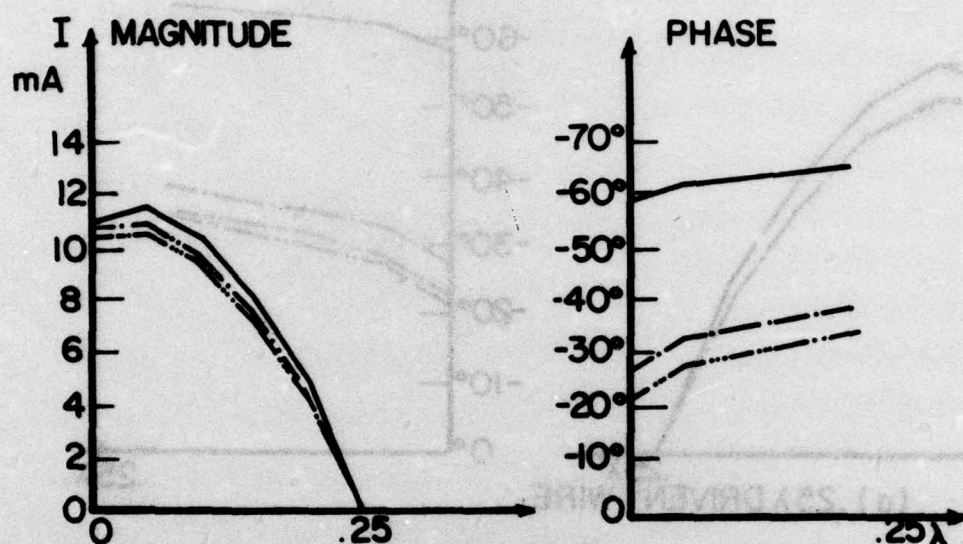
FIG.13   CURRENT DISTRIBUTION .25 λ TO .75 λ

16

quite regular for all lengths, $L \leq .5\lambda$.

The normalized maximum parasite currents as a function of d for $L = .125\lambda$, $.166\lambda$, $.25\lambda$, $.375\lambda$, and $.5\lambda$ are summarized in Fig. 14 with d changing from $.1\lambda$ to 2.0λ. From this plot it is seen that the change in the current magnitude with d closely resembles K/d as shown in Fig. 15, if the proper value of K is selected. The phase change for the steps $\Delta d = .1\lambda$ is nearly constant and equal to 36° for $d > .5\lambda$. Even for values of d smaller than $.5\lambda$ the deviation is quite acceptable for radiation pattern purposes.

After some experimenting, we found that, for L in the range of values studied, for $d \geq .8\lambda$ the magnitude and phase of the parasite current distribution are uniform and inversely proportional to d. We can relate the currents for $d \geq .8\lambda$ to their computed value at $d = .8\lambda$ by the following simple relations.

$$|I|(d) = \frac{K}{(d/\lambda)}$$

$$\theta(d) = \frac{2\pi}{\lambda} (d - .8\lambda) + \theta(.8\lambda)$$

(1)

where K is a constant to be determined from

$$\frac{K}{.8} = |I|(.8\lambda)$$

where $|I|(.8\lambda)$ is the current magnitude at $d = .8\lambda$

$\theta(.8\lambda)$ is phase of the current at $d = .8\lambda$.

As an example for $L = .125\lambda$, $K = 2.24$ and Fig. 16 shows in the solid line a plot of curve (1) of Fig. 14 and in the X's, the computed values for $|I|(d) = 2.24/(d/\lambda)$. The agreement is very good indeed. Similar results are obtained for the other values of L. The representation is especially good for $d \geq .8\lambda$.

5. Equivalent Point Source

The parasite wire current can be obtained for any value of d by using MOM

Imax

1.0

.8

.6

FOR (1) L = .125 λ
(2) L = .166 λ
(3) L = .25 λ
(4) L = .375 λ
(5) L = .5 λ

.4
(4)(2)   (1)

(5)

.2
(3)

0
.4   .8   1.2   1.6   2.0
d/λ

Δφ°
PHASE CHANGE FOR Δd=.1λ

-50°

-40°   o(2)

-30°   (1)°

-20°

-10° (5)°
      (4)

0   (3)
0   .4   .8   1.2   1.6   20
d/λ
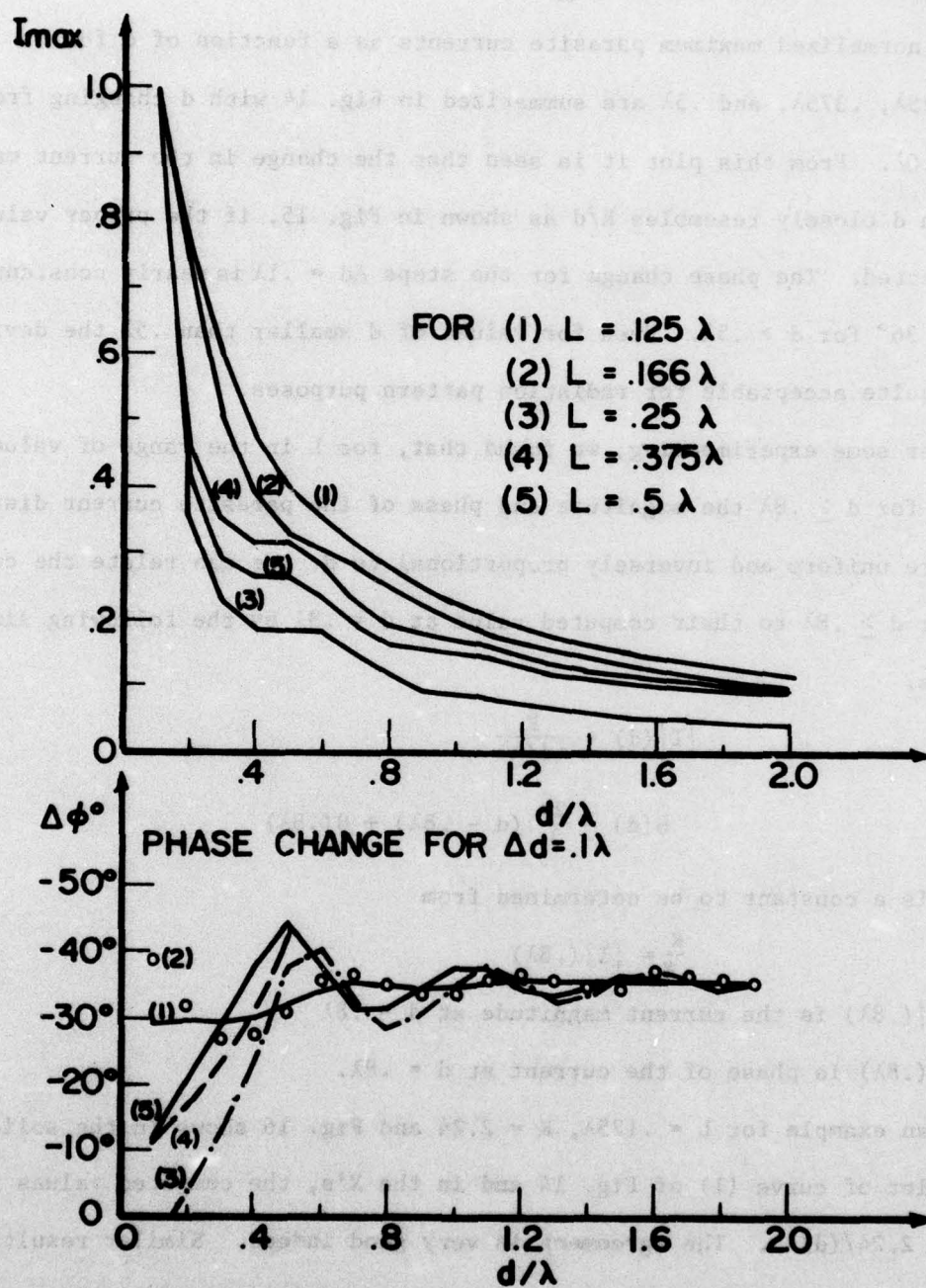
FIG. 14 NORMALIZED MAXIMUM PARASITE CURRENT AND PHASE
AS A FUNCTION OF d/λ

FIG. I5   THE VARIOUS CURVES OF K/d

19
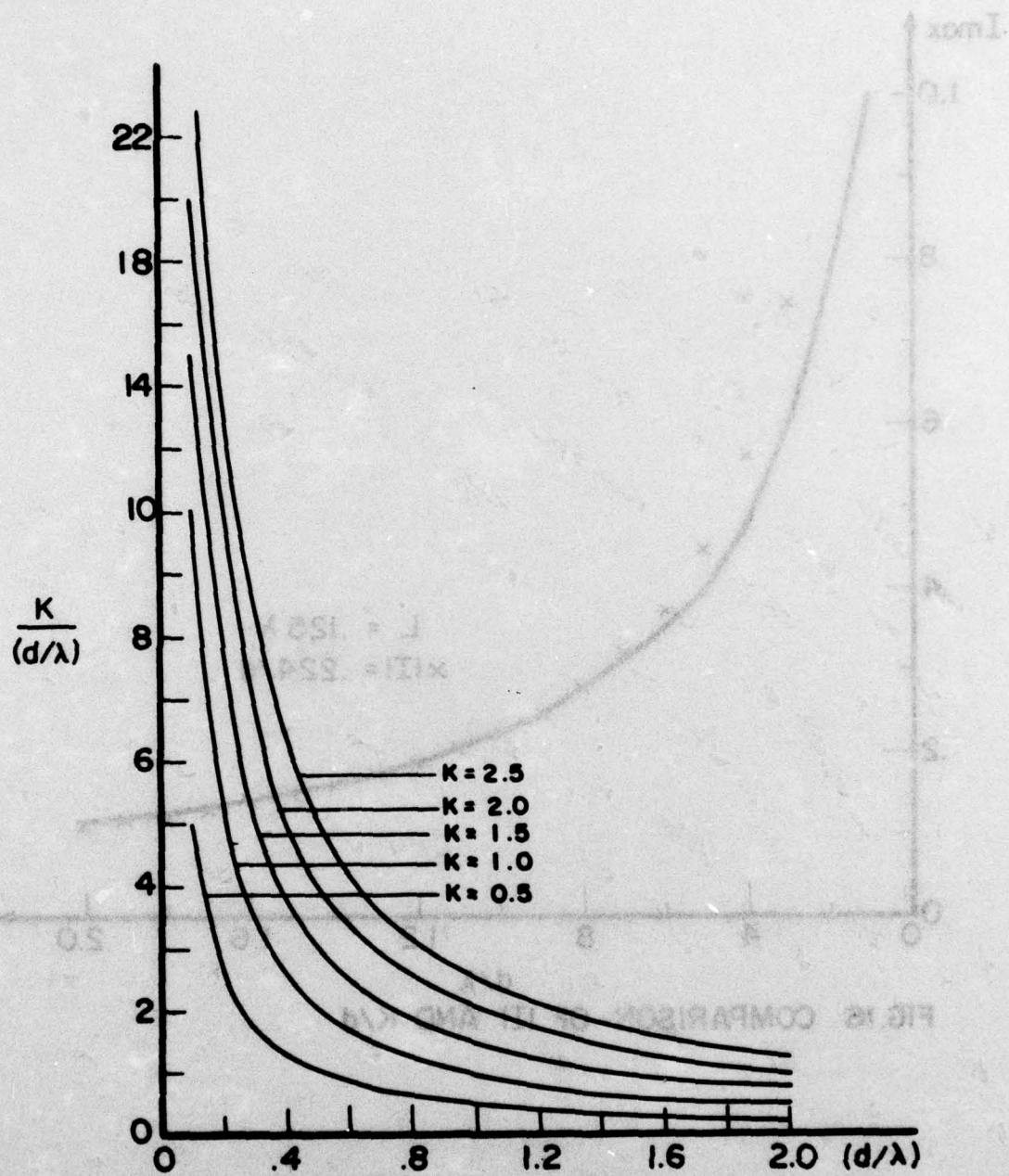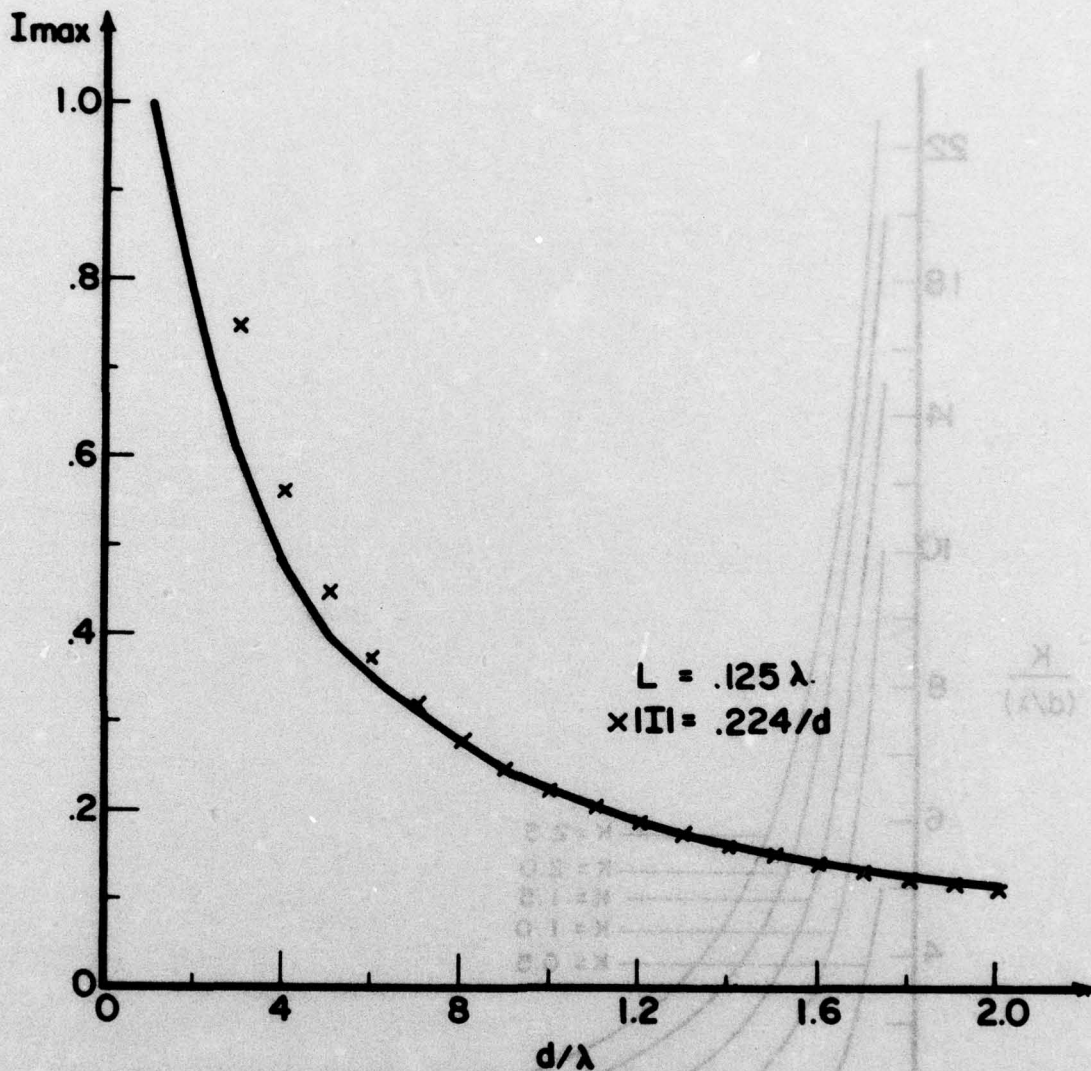
FIG.16 COMPARISON OF |I| AND K/d

FIG.15 THE VARIOUS CURVES OF K/d

once for $d = .8\lambda$ and equations (1). After the current is obtained for every parasite wire of Fig. 2, each wire can be treated as a point source I_p by summing the phasor contribution of each current element in the desired angle as shown in Fig. 17 by the equation

$$I_p = \sum_{i=0}^{N} I_i e^{j\left(\frac{2\pi \ell_i \sin\theta}{\lambda} + \theta_i\right)}$$

After all equivalent point sources have been obtained, the problem of Fig. 2 can be treated by the synthesis program referred to in section 1 [1] as a planar array of point sources.

6. Conclusions and Recommendations.

It seems that the hypotheses set forth in the introduction of this report have been satisfactorily verified. Before we proceed and apply these results to the problem of optimizing the antenna site on ships, we would like to verify further the hypothesis set forth by Raschke and Sterling [2] and stated in section 2 of this report. The computations made by them referred to infinitely long cylinders. We would like to use the body of revolution computer program [4] and MOM program to check the same hypothesis for finite size cylinders. The influence of the wire separation S, the number of wires, and wire radius can be very easily studied with the use of these codes.

References

[1] Perini, J., Idselis, M.M., "Point Source Radiation Pattern Synthesis by Iterative Techniques," NAVY Report (to be published).

[2] Raschke, R.R., Sterling, J.T., Final Engineering Report: Linear Antenna Pattern Prediction Model Development, Contract N00024-73C-1277, Space Systems, General Electric Co., Daytona Beach, Florida.

FIG. 17 EQUIVALENT POINT SOURCE

[3] Perini, J., Internal letter to Raschke.

[4] Mautz, J.R., Harrington, R.F., "Radiation and Scattering from Bodies of Revolution," App. Sci. Res., Vol. 20, June 1969.

METRIC SYSTEM

BASE UNITS:

Quantity	Unit	SI Symbol	Formula
length	metre	m	...
mass	kilogram	kg	...
time	second	s	...
electric current	ampere	A	...
thermodynamic temperature	kelvin	K	...
amount of substance	mole	mol	...
luminous intensity	candela	cd	...

SUPPLEMENTARY UNITS:

plane angle	radian	rad	...
solid angle	steradian	sr	...

DERIVED UNITS:

Acceleration	metre per second squared	...	m/s
activity (of a radioactive source)	disintegration per second	...	(disintegration)/s
angular acceleration	radian per second squared	...	rad/s
angular velocity	radian per second	...	rad/s
area	square metre	...	m
density	kilogram per cubic metre	...	kg/m
electric capacitance	farad	F	A·s/V
electrical conductance	siemens	S	A/V
electric field strength	volt per metre	...	V/m
electric inductance	henry	H	V·s/A
electric potential difference	volt	V	W/A
electric resistance	ohm		V/A
electromotive force	volt	V	W/A
energy	joule	J	N·m
entropy	joule per kelvin	...	J/K
force	newton	N	kg·m/s
frequency	hertz	Hz	(cycle)/s
illuminance	lux	lx	lm/m
luminance	candela per square metre	...	cd/m
luminous flux	lumen	lm	cd·sr
magnetic field strength	ampere per metre	...	A/m
magnetic flux	weber	Wb	V·s
magnetic flux density	tesla	T	Wb/m
magnetomotive force	ampere	A	...
power	watt	W	J/s
pressure	pascal	Pa	N/m
quantity of electricity	coulomb	C	A·s
quantity of heat	joule	J	N·m
radiant intensity	watt per steradian	...	W/sr
specific heat	joule per kilogram-kelvin	...	J/kg·K
stress	pascal	Pa	N/m
thermal conductivity	watt per metre-kelvin	...	W/m·K
velocity	metre per second	...	m/s
viscosity, dynamic	pascal-second	...	Pa·s
viscosity, kinematic	square metre per second	...	m/s
voltage	volt	V	W/A
volume	cubic metre	...	m
wavenumber	reciprocal metre	...	(wave)/m
work	joule	J	N·m

SI PREFIXES:

Multiplication Factors	Prefix	SI Symbol
1 000 000 000 000 = 10^{12}	tera	T
1 000 000 000 = 10^9	giga	G
1 000 000 = 10^6	mega	M
1 000 = 10^3	kilo	k
100 = 10^2	hecto*	h
10 = 10^1	deka*	da
0.1 = 10^{-1}	deci*	d
0.01 = 10^{-2}	centi*	c
0.001 = 10^{-3}	milli	m
0.000 001 = 10^{-6}	micro	μ
0.000 000 001 = 10^{-9}	nano	n
0.000 000 000 001 = 10^{-12}	pico	p
0.000 000 000 000 001 = 10^{-15}	femto	f
0.000 000 000 000 000 001 = 10^{-18}	atto	a

* To be avoided where possible.

MISSION
of
Rome Air Development Center

RADC plans and conducts research, exploratory and advanced development programs in command, control, and communications (C^3) activities, and in the C^3 areas of information sciences and intelligence. The principal technical mission areas are communications, electromagnetic guidance and control, surveillance of ground and aerospace objects, intelligence data collection and handling, information system technology, ionospheric propagation, solid state sciences, microwave physics and electronic reliability, maintainability and compatibility.